Proc. of the European Safety and Reliability Conference (ESREL 2026)
Edited by José C. Matos, Paulo B. Lourenço, Michael Beer, Daniel Oliveira, Edoardo Patelli, Hélder S. Sousa, Rui A. Silva and Monica Santamaria

doi: 10.3850/ESREL2026061419_esrel26-p26084-cd

Non-stationary analysis of the date of ice breaking in the ice classic of Nenana river (Alaska)

Patricia Mares-Nasarre

Department of Hydraulic Engineering, Delft University of Technology, the Netherlands.
E-mail: p.maresnasarre@tudelft.nl

Stuart G. Pearson

Department of Hydraulic Engineering, Delft University of Technology, the Netherlands.
E-mail: s.g.pearson@tudelft.nl

Kieran B.J. Dunne

Department of Hydraulic Engineering, Delft University of Technology, the Netherlands.
E-mail: k.b.j.dunne@tudelft.nl

Robert Lanzafame

GEI Consultants, 180 Grand Ave Suite 950, Oakland, California USA, 94612
E-mail: *rlanzafame@geiconsultants.com*

The Nenana Ice Classic is an annual event in Nenana, Alaska, which functions as a community fundraiser where participants wager on the precise date and time (hour and minute) of the spring breakup of the Tanana River ice at Nenana. Beyond its cultural and fundraising role, ice breakup in northern rivers is closely related with the formation of ice jams, which can rapidly dam river flow and lead to severe flooding in adjacent communities. Historical records of the ice breakup of the Tanana River ice are available since 1917. Here, the time of ice breakup relative to 1st January every year is analyzed. A significant linear decreasing trend is found while the residuals are found to be homoscedastic. A non-stationary distribution using time as a covariate is used to model uncertainty in the data and estimate probabilities to find the breakup date before the wagering day date for different time scenarios. In addition, several climatic covariates are analyzed as possible contributors to uncertainty in the breakup date, including air temperature, the discharges in the river or the cloud coverage, amongst others.

Keywords: non-stationary, ice breakup, Nenana Ice Classic, covariates.

1. Introduction: Nenana Ice Classic

The Nenana Ice Classic, an ”Alaskan Tradition,” is an annual fundraising event that takes place in the small community of Nenana, Alaska. Participantswager on the exact day, hour, and minute when spring breakup of the Tanana River ice will occur, with a chance to win a cash prize up to several hundred thousand US dollars. Each year, during the first weekend of March, a wooden tripod is constructed and anchored to the ice in the Tanana River at Nenana. The tripod is connected via a rope to a shore-based clock tower complete with a weighted cable-and-pulley system. When the ice sheet weakens and the tripod is carried downstream approximately 30 meters (100 feet), tension in the rope activates a mechanism that halts the clock, setting the official breakup time with minute-level precision. Beyond its important cultural and fundraising role in Nenana and Alaska, ice breakup in northern rivers is closely related to the formation of ice jams, which can rapidly dam river flow and lead to severe flooding in adjacent communities (Lindenschmidt et al., 2018). The historical records of the ice breakup of the Tanana River ice therefore present an opportunity to learn about the natural phenomena influencing ice breakup, as a complete record is available at this location since 1917.

The contribution of this study is two fold: (1) the evolution of river ice breakup date over time is analyzed, and (2) the covariates that better explain this phenomenon are identified and implemented in a probabilistic model. To do so, first, the time and date of ice breakup in the Tanana River is analyzed as a function of time using non-stationary analysis. Afterwards, covariates are explored using rank correlations and forward stepwise linear regression. Finally, the date of the ice break is modelled using non-parametric Bayesian Networks (NPBN).

2. Materials and Methods

2.1. *Datasets*

The time and date of the ice breakup in the Tanana River at Nenana, Alaska (USA) is defined as the number of hours, $hours$, relative to 00:00 on the 1st of January in a given year until the ice breakup time recorded in that year by the Nenana Ice Classic competition. These data are available online (Nenana Ice Classic, 2020).

The following physical variables are also considered in the analysis:

- Cloud coverage, $cloud$ ($\%$), fraction of the sky obscured by clouds. Here, monthly average is used
  and data was retrieved from University of East Anglia Climatic Research Unit et al. (2020) for the coordinates ($64.75° N, -149.25° E$)
- River discharge, q (ft^3/s), average monthly volume of water per unit of time that flows in the Tanana River. Here, the monthly average was used and data was retrieved from USGS (2020).
- Southern Oscillation Index, SOI (-), standardized index based on the observed sea level pressure between Tahiti and Darwin (Australia) that measures large-scale fluctuations in air pressure. Monthly data was retrieved from NOAA (2025). Previous studies (Papineau, 2001) have found modest or weak relationships between the winter temperature and sea ice cover in Alaska and SOI.
- Arctic Oscillation, AO (-), standardized index based on the atmospheric pressure differences between the Arctic and mid-latitudes, indicating shifts in the polar vortex and jet stream. Studies such as Bond and Harrison (2006) indicate that the joint effect of AO and SOI can describe the weather variability in Alaska. Monthly data was retrieved from NOAA (2025).
- Pacific Decadal Oscillation, PDO (-), long-lived El Niño-like pattern of Pacific climate variability (Zhang et al., 1997) which typically lasts between 20 and 30 years and influences temperature and precipitation in Alaska (Wendler et al., 2017). Monthly data was retrieved from NOAA (2025).
- Pacific-North American Oscillation, PNA (-), standardized index based on the atmospheric pressure differences between the North Pacific and North America. L'Heureux et al. (2004) showed a significant relationship between precipitation in Alaska and PNA. Monthly data was retrieved from NOAA (2025).
- North Atlantic Oscillation, NAO (-), oscillation of atmospheric pressure between the Azores High (low pressure) and the Icelandic Low (high pressure) over the North Atlantic, which influences winter weather across the Northern Hemisphere. NAO mainly influences weather in Europe and the eastern U.S. Monthly data was retrieved from NOAA (2025).
- Cumulative monthly precipitation, P (mm/month). The dataset is described in Harris et al. (2020) and was retrieved from University of East Anglia Climatic Research Unit et al. (2020) in the coordinates ($64.75° N, -149.25° E$).
- Monthly and daily average, minimum and maximum surface temperature, T_m, T_d, $T_{d,min}$, $T_{d,max}$ ($°C$), retrieved from Rohde and Hausfather (2020).
- Ice thickness, h (cm), measured at Nenana and retrieved from Nenana Ice Classic (2024).

Observations between January and March each year are selected. All physical variables except T_d, $T_{d,min}$ and $T_{d,max}$ are monthly. For T_d, $T_{d,min}$ and $T_{d,max}$, the number of days over $0°C$ ($N_{days,avg}$, $N_{days,min}$ and $N_{days,max}$, respectively) and the cumulative excess of temperature over $0°C$ (E_{avg}, E_{min}, and E_{max}, respectively) during January, February, and March are computed. For the variables with monthly resolution, the following covariates are defined: the minimum and the maximum of the period, and the gradient, computed as the slope of the linear regression of the three observations of January, February and March.

2.2. *Non-stationary analysis*

2.2.1. *Data inspection*

The timeseries of $hours$ is first visually inspected (see Figure 1). In this study, the observed trend is modelled with a linear regression and statistically tested using Mann-Kendall test (Mann, 1945; Kendall, 1975) with null hypothesis that there is no trend in the data. Note that observations in this study can be assumed independent as one observation per year is considered. Heteroscedasticity is also tested using the White test (White, 1980): whether the variance of the residuals, defined as the difference between the observations and the trend, is constant across all observations. The null hypothesis of this test corresponds to equal variance in the residuals, namely homoscedasticity.

2.2.2. *Covariate selection*

In order to assess the explanatory power of the defined covariates, Spearman's rank correlation r is used. $r \in [-1, 1]$, where r=1 and -1 correspond to a perfect positive and negative monotonic dependence, respectively. $p-values$ associated with r are also computed to assess the significance of the observed correlations. Covariates with significant r with $hours$ are selected for further analysis. If two covariates with significant correlation with $hours$ have a very strong positive correlation between them ($r > 0.9$), the covariate with the lowest correlation with $hours$ is discarded.

2.2.3. *Detrending approach*

Covariates found to be significant and homoscedastic in the previous tests are detrended using a linear regression fit (described in Section 2.2.4). Therefore, the timeseries X_c is separated into a deterministic, $D(c)$, and a stochastic component, Y_c, as $X_c = D(c) + Y_c = S\,c + I + Y_c$, where c denotes a given time or a value of a covariate, S and I are the slope and intercept obtained from the linear regression. Y_c is modelled using a parametric continuous distribution function. The goodness of fit of the selected distribution is tested using the one-sample Anderson-Darling test (Stephens, 1974, 1976), whose null hypothesis is that the sample follows the selected distribution. Therefore, for $Y_c \sim F$, return levels of X_c for a given value of c and non-exceedance probability p, $Z_X(c,p)$, can be estimated as $Z_X(c,p) = S\,c + I + F^{-1}(p)$.

2.2.4. *Regression with covariates*

In order to assess the explanatory power of the covariates and build an "order of importance", a forward stepwise regression is applied (e.g. Mares-Nasarre et al., 2021). To do so, linear trends are assumed between $hours$ and the covariates described in Section 2.1. The covariates are introduced one by one in the linear regression to assess which covariate explains the highest percentage of variance. First, models composed of a constant and one of the covariates are built; the percentage of variance explained by each model is roughly assessed through the coefficient of determination, R^2. The covariate whose regression provides the highest R^2 is kept. Linear regression is then performed using a constant, the covariate selected in the previous step, and an additional covariate from those not yet included in the regression model. This procedure is repeated until incorporation of an additional covariate does not significantly improve the model according to the adjusted coefficient of determination (R^2_{adj}) defined by Theil (1961) as

$$R^2_{adj} = 1 - (1 - R^2)\frac{N-1}{N-N_p-1} \qquad (1)$$

where N is the number of observations and N_P is the number of covariates included in the regression. The procedure is stopped when adding a covariate does not improve R^2_{adj}.

2.3. *Non-parametric Bayesian Networks*

Bayesian Networks (Pearl, 2013) are multivariate probability distribution functions in high dimensions composed by a Directed Acyclic Graph

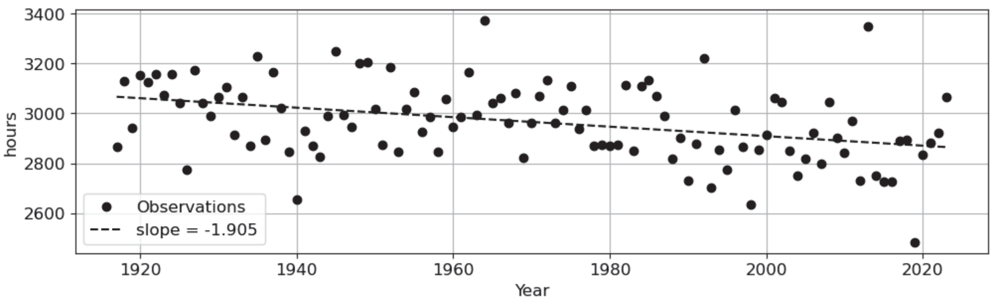

Fig. 1. Time series of the number of hours from 1st January until the ice breakup time each year, $hours$ and linear trend using $Year$ as covariate.

(DAG) which consists of a set of nodes and a set of arcs. Each node represents a random variable, and each arc connects two nodes and indicates probabilistic dependence. Therefore, a Bayesian Network encodes the joint probability density on a set of variables by specifying conditional probability functions of each variable (child) given its direct preceding variables (parents). Here, non-parametric Bayesian Networks or copula-based Bayesian Networks (NPBNs) as defined by Hanea et al. (2006) and Hanea et al. (2015) are used: empirical univariate distributions quantify the nodes while bivariate Gaussian copulas are used to model the dependence between each pair of random variables. NPBNs are implemented using the Python library BANSHEE (Koot et al., 2023).

In order to validate the assumption of the Gaussian copula, the empirical rank correlation matrix computed from the observations using Eq. (**??**), R_E, is compared with the rank correlation matrix corresponding to the saturated model, R_S, where all the nodes are connected to each other. R_S represents the best possible model achievable with a NPBN in terms of performance. Therefore, if R_E and R_S are similar, a NPBN is able to capture the dependence structure of the data. It should be noted that R_S does not explain the underlying physics as all nodes are connected to each other. Thus, here, a non-saturated DAG is proposed. The rank correlation matrix of that DAG, R_{BN}, is computed using the protocol in Hanea et al. (2006) and compared with R_S to assess how "far" the proposed DAG is from the best achievable model. In order to perform these comparisons, the d-calibration score, $d(R_1, R_2)$, proposed in Morales-Nápoles et al. (2013) is used.

$d(R_1, R_2)$ assesses the "distance" between the elements of the two correlation matrices. If matrices are identical, the score is 1, while it becomes closer to 0 as matrices differ from each other element-wise.

3. Results

3.1. *Non-stationary analysis over time*

As shown in Figure 1, a negative trend is visible on $hours$ over time ($Year$), which is significant according to the Man-Kendall test (see Section 2.2.1) with slope $S_t = -1.905$ hours/year and intercept $I_t = 6719.04$ hours.

Residuals R_t are computed by deducting the linear trend from the observations (see Section 2.2.3). R_t are found homocedastic and are fitted to a Gaussian distribution, such that $R_t \sim \Phi(-4.6 \cdot 10^{-13}, 142.9)$ (units $hours$). The goodness of fit of this distribution is tested using the one-sample Anderson-Darling test, whose null hypothesis is that the sample follows a Gaussian distribution. The null hypothesis cannot be rejected with a significance of 0.05.

Using this model, the probability of ice breaking before a specific day and time can be computed for a specific year. Noting that the deadline for placing the wager is April 5th, for example, in the year 1920, close to the year of the first historical record, P[$hours$ < wagering time in 1920] = $2.3 \cdot 10^{-8}$. In contrast, for the year 2030, P[$hours$ < wagering time in 2030] = $3.2 \cdot 10^{-5}$, showing a change of three orders of magnitude. The distributions of $hours$ for years 1920 and 2030 are shown in Figure 2.

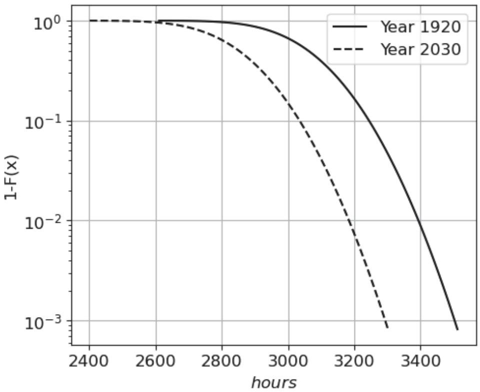

Fig. 2. Inverse Cumulative Distribution Function in semi-log scale of hours from January 1 until breakup time each year, $hours$, for the years 1920 and 2030. Note there are 2255 hours between January 1 and the betting deadline of April 5.

One of the risks for the organizers of the Ice Classic competition is that ice breaks before the deadline to place the wagers has passed. In other words, what is $P[hours < 2255]$, and how could this change in future years? If the organizers would like to maintain the status quo of 1920, P[$hours$ < wagering time in 2030] = P[$hours$ < wagering time in 1920] = $2.3 \cdot 10^{-8}$, the deadline for placing the wagers would need to be moved forward 7.7 days to March 28. Finally, if the observed trend is assumed to persist in the future, the year in where this probability becomes 0.01, P[$hours$ < wagering time]$> 10^{-2}$, is found to be 2168.

Although this model is useful for gaining insight into changes of the probability distribution of $hours$ over time, the standard deviation is $\frac{142.9\ hours}{24} = 5.95$ days, corresponding to a 90% interquantile range of 19.6 days. Therefore, the model predicts a significant uncertainty in $hours$, and does not provide additional insight to the underlying physical phenomenon (i.e., we cannot rely on this information alone to win the competition). Thus, in the following sections, covariates are evaluated with the purpose of finding potentially significant physical explanators of the ice breaking.

3.2. *Non-stationary analysis with covariates*

Following the methodology described in Section 2.2.2, 9 covariates are selected: maximum q (q_{max}), maximum SOI (SOI_{max}), maximum precipitation (P_{max}), maximum T_m (T_{max}), maximum PDO (PDO_{max}), minimum h (h_{min}), minimum PNA (PNA_{min}), minimum NAO (NAO_{min}), and $N_{days,avg}$. The rank correlation matrix of the selected variables is shown in Figure 3.

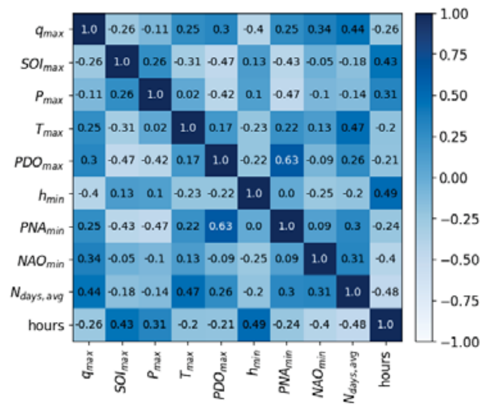

Fig. 3. Empirical rank correlation matrix of $hours$ and selected covariates.

The aforementioned variables are used as input for the regression procedure described in Section 2.2.4. Note that the observation period for each covariate is different; however, there is a 30 year period where data for all covariates is available. Variables are included in the regression model in the following order: h_{min}, SOI_{max}, $N_{days,avg}$, P_{max}, PNA_{min}, and q_{max}. The goodness of fit of the regression model is $R^2 = 0.63$.

This regression model is used to detrend the observations of $hours$ and obtain residuals R_c. R_c are homocedastic and present a standard deviation of $\frac{95.08\ hours}{24} = 3.96$ days; the 90% interquantile range is 16.6 days.

3.3. *Joint distribution with NPBNs*

A NPBN is built using the 9 covariates selected using the methodology in Section 2.2.2 and the variable of interest, $hours$. The DAG displayed in Figure 4 is proposed.

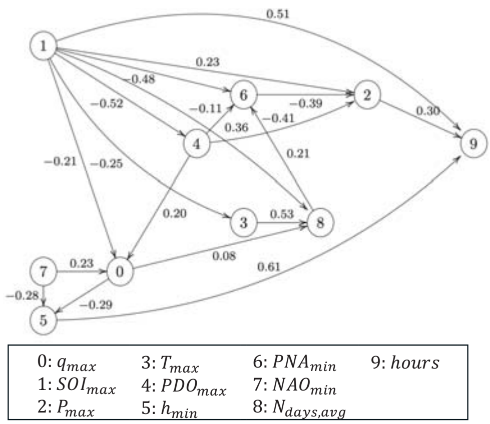

Fig. 4. Proposed DAG for the BN. Covariates (variables) are identified by numbered circles (nodes) and arcs are labelled with the (un)conditional rank correlations between two nodes.

Validation of the Gaussian copula assumption and the proposed DAG in Figure 4 is conducted as exposed in Section 2.3; $d(R_E, R_S) = 0.81$ and $d(R_{BN}, R_S) = 0.58$. The Gaussian copula assumption seems reasonable according to the $d(R_E, R_S) = 0.81$, which is close to 1. The proposed DAG in Figure 4 also presents a reasonable performance being relatively close to R_S.

In order to assess the predictive power of the NPBN, an in-sample validation is conducted. The values of the 9 selected covariates are used to conditionalize the NPBN and estimate the conditional distribution of $hours$, $F(hours|q_{max}, SOI_{max}, P_{max}, T_{max}, PDO_{max}, h_{min}, PNA_{min}, NAO_{min}, N_{days,avg})$. Figure 5 presents the observations of $hours$ in comparison with the 5%, 50% and 95% percentiles of $F(hours|q_{max}, SOI_{max}, P_{max}, T_{max}, PDO_{max}, h_{min}, PNA_{min}, NAO_{min}, N_{days,avg})$; 3 out of 30 observations fall outside the 90% interval.

Using $F(hours|q_{max}, SOI_{max}, P_{max}, T_{max}, PDO_{max}, h_{min}, PNA_{min}, NAO_{min}, N_{days,avg})$ computed for each observation, the 90% interquantile distance and standard deviation are calculated. The 90% interquantile distance varies between 8.9 and 21.2 days with an average of 14.7 days. The standard deviation ranges from 2.8 to 7.1 days with an average of 4.6 days.

4. Discussion

Several probabilistic techniques are used to explain the ice breakup day and time observed in the Tanana River, Alaska. First, a non-stationary approach using time as a covariate is applied. A significant decreasing linear trend over time (i.e., breakup dates generally occurring earlier in the year over time) was found. As also found in previous studies on sea ice (e.g.: Liu et al., 2020), we hypothesize this may be due to climate change. Extrapolating with the linear non-stationary trend allows inferences to be made regarding scenarios in the future. However, the choice of a linear trend is purely based on historical data and should be treated with care, as there is no evidence of that such a trend will continue in the future.

The second part of this analysis uses a number of covariates (Section 2.1) to explain the trend and uncertainty of breakup day and time. An initial set of 9 covariates is selected based on rank correlation with breakup, r (see Section 2.2.2): q_{max}, SOI_{max}, P_{max}, T_{max}, PDO_{max}, h_{min}, PNA_{min}, NAO_{min}, and $N_{days,avg}$. Using regression, the set of covariates is reduced and ordered based on individual percentage contributions to the variance (see Section 2.2.4), specifically: h_{min}, SOI_{max}, $N_{days,avg}$, P_{max}, PNA_{min}, and q_{max}.

According to Beltaos (2003), there are two mechanisms for river ice breakup, namely mechanical and thermal. Mechanical breakup is controlled primarily by river discharge, explaining why q_{max} is found to have a significant contribution. Thermal breakup is controlled primarily by temperature. Here, $r(hours, T_{max})$ and $r(hours, N_{days,avg})$ are found to be significant, and $N_{days,avg}$ is also included in the reduced subset. We hypothesize that this is due to the

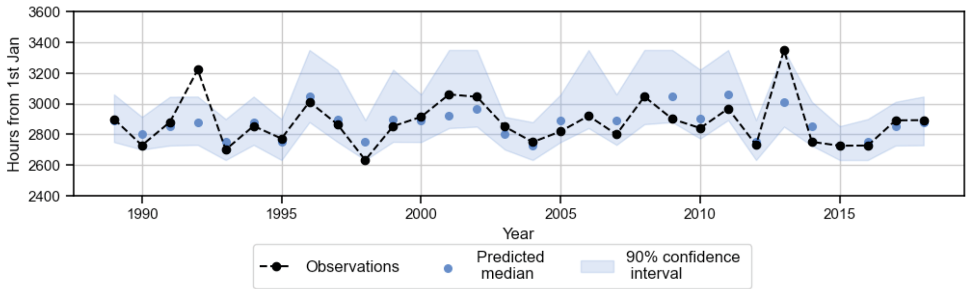

Fig. 5. In-sample validation of NPBN with Gaussian copula assumption.

persistence of a given temperature being more important for ice melt than the value of a strong, but short-term, peak value. We believe that this is also why $N_{days,avg}$ is included in the reduced subset instead of T_{max} and why $r(hours, N_{days,avg}) > r(hours, N_{days,min})$ and $r(hours, N_{days,avg}) > r(hours, N_{days,max})$. Future research could assess these correlations once ice breakup events are classified and separated by mechanism, as it might lead to stronger correlations.

A relation between PNA_{min} precipitation in Alaska has previously been found (L'Heureux et al., 2004) and both PNA_{min} and P_{max} are included in the reduced subset. We believe that precipitation may act as a proxy for snow pack which is, in turn, related to river discharge. It should be noted that P_{max}, PNA_{min}, and q_{max} are based on monthly data, which might explain why the three variables are needed to better capture the oscillations in $hours$.

SOI_{max} is found to be the covariate that explains the highest percentage of variance. However, weak correlations between SOI and winter temperature and ice cover in Alaska have been previously reported (Papineau, 2001). High values of SOI correspond to "La Niña" episodes with cooler-than-normal ocean temperatures in the eastern Pacific. We hypothesize that this global oscillation becomes relevant due to the low resolution of some climatic variables (e.g.: P_{max}) or the lack of observations of some relevant climatic variables (e.g.: snow pack).

Results in this research should be treated with care as most of the methods applied require paired observations. The datasets incorporated in the analysis only overlap for 30 years, which is a limited sample. Future research could validate the conclusions of this study using applications with more data available. Also, the NPBN was built using the 9 covariates selected based on r, as the method builds on correlations. However, it might be possible to reduce the number of covariates included in the NPBN while achieving the same performance.

5. Conclusions

This research has analyzed the temporal trend of ice breakup date in the Tanana River next to Nenana, Alaska, and has identified potential covariates that help to explain this complex natural phenomenon. A NPBN has been proposed to model joint dependence of 9 covariates and the ice breakup date achieving 90% interquantile ranges between 8.9 and 21.2 days. This model might be used to narrow down the prediction of a time window when ice breakup may occur and help responsible organizations optimize resources to prevent or mitigate flood damages due to ice breakup events.

Analytic methods and procedures used in this research can be used in many other time-dependent phenomena with a high degree of uncertainty from numerous covariates. As such, data and code used in this research are shared under a CC BY 4.0 license at https://doi.org/10.5281/zenodo.18098030

Acknowledgement

The authors would like to acknowledge the conversations with numerous students and colleagues at the Civil Engineering and Geosciences Faculty of Delft University of Technology, especially via MUDE, that helped motivate the analysis described in this paper: perhaps this is our lucky year!

References

Beltaos, S. (2003). Threshold between mechanical and thermal breakup of river ice cover. *Cold Regions Science and Technology 37*(1), 1–13.

Bond, N. A. and D. E. Harrison (2006). Enso's effect on alaska during opposite phases of the arctic oscillation. *International Journal of Climatology 26*(13), 1821–1841.

Hanea, A. M., D. Kurowicka, and R. M. Cooke (2006). Hybrid method for quantifying and analyzing bayesian belief nets. *Quality and Reliability Engineering International 22*(6), 709–729.

Hanea, A. M., O. Morales Nápoles, and D. A. Ababei (2015). Non-parametric bayesian networks: Improving theory and reviewing applications. *Reliability Engineering & System Safety 144*, 265–284.

Harris, I., T. J. Osborn, P. Jones, and D. Lister (2020). Version 4 of the cru ts monthly high-resolution gridded multivariate climate dataset. *Scientific Data 7, 109*.

Kendall, M. G. (1975). *Rank Correlation Methods*. 4th edition, Charles Griffin, London.

Koot, P., M. A. Mendoza-Lugo, D. Paprotny, O. Morales-Nápoles, E. Ragno, and D. T. Worm (2023). Pybanshee version (1.0): A python implementation of the matlab toolbox banshee for non-parametric bayesian networks with updated features. *SoftwareX 21*, 101279.

L'Heureux, M. L., M. E. Mann, B. I. Cook, B. E. Gleason, and R. S. Vose (2004). Atmospheric circulation influences on seasonal precipitation patterns in alaska during the latter 20th century. *Journal of Geophysical Research: Atmospheres 109*(D6).

Lindenschmidt, K.-E., M. Huokuna, B. C. Burrell, and S. Beltaos (2018). Lessons learned from past ice-jam floods concerning the challenges of flood mapping. *International Journal of River Basin Management 16*(4), 457–468.

Liu, Y., J. R. Key, X. Wang, and M. Tschudi (2020). Multidecadal arctic sea ice thickness and volume derived from ice age. *The Cryosphere 14*(4), 1325–1345.

Mann, H. B. (1945). Nonparametric tests against trend. *Econometrica 13*(3), 245–259.

Mares-Nasarre, P., J. Molines, M. E. Gómez-Martín, and J. R. Medina (2021). Explicit neural network-derived formula for overtopping flow on mound breakwaters in depth-limited breaking wave conditions. *Coastal Engineering 164*, 103810.

Morales-Nápoles, O., A. M. Hanea, and D. Worm (2013). Experimental results about the assessments of conditional rank correlations by experts: Example with air pollution estimates. In *Proceedings 22nd European Safety and Reliability Conference "Safety, Reliability and Risk Analysis: Beyond the Horizon", ESREL 2013, Amsterdam, the Netherlands, 29–9 to 2–10*. Taylor & Francis Group, London.

Nenana Ice Classic (2020). Nenana ice classic: Tanana river ice annual breakup dates, version 2. NASA National Snow and Ice Data Center Distributed Active Archive Center.

Nenana Ice Classic (2024). Ice measurements. Nenana Ice Classic.

NOAA (2025). Climate monitoring. National Centers for Environmental Information. National Oceanicand Athmospheric Administration.

Papineau, J. M. (2001). Wintertime temperature anomalies in alaska correlated with enso and pdo. *International Journal of Climatology 21*(13), 1577–1592.

Pearl, J. (2013). A constraint propagation approach to probabilistic reasoning.

Rohde, R. A. and Z. Hausfather (2020). The berkeley earth land/ocean temperature record. *Earth System Science Data 12*(4), 3469–3479.

Stephens, M. A. (1974). EDF statistics for goodness of fit and some comparisons. *Journal of the American Statistical Association 69*(347), 730–737.

Stephens, M. A. (1976). Asymptotic results for goodness-of-fit statistics with unknown parameters. *The Annals of Statistics 4*(2), 357–369.

Theil, H. (1961). *Economic Forecasts and Policy*. North, Amsterdam (Holland).

University of East Anglia Climatic Research Unit, P. D. Jones, and H. I. C (2020). Climatic research unit (cru): Time-series (ts) datasets of variations in climate with variations in other phenomena v4. Centre for Environmental Data Analysis.

USGS (2020). Tanana R at Nenana AK - 15515500. United States Geological Survey River Monitoring Location.

Wendler, G., T. Gordon, and M. Stuefer (2017). On the precipitation and precipitation change in alaska. *Atmosphere 8*(12).

White, H. (1980). A heteroskedasticity-consistent covariance matrix estimator and a direct test for heteroskedasticity. *Econometrica 48*(4), 817–838.

Zhang, Y., J. M. Wallace, and D. S. Battisti (1997). Enso-like interdecadal variability: 1900–93. *Journal of Climate 10*(5), 1004 – 1020.